

# THE HYTI MISSION

**Robert Wright<sup>(1)</sup>, Paul Lucey<sup>(1)</sup>, Miguel Nunes<sup>(2)</sup>, Sarath Gunapala<sup>(3)</sup>, Sir Rafol<sup>(3)</sup>, David Ting<sup>(3)</sup>, Luke Flynn<sup>(1)</sup>, Chiara Ferrari-Wong<sup>(1)</sup>, Alexander Soibel<sup>(3)</sup>, Thomas George<sup>(4)</sup>**

<sup>(1)</sup>*Hawai‘i Institute of Geophysics and Planetology, University of Hawai‘i at Mānoa, 1680 East-West Road, Honolulu, HI, U.S.A.*

<sup>(2)</sup>*Hawai‘i Space Flight Laboratory, University of Hawai‘i at Mānoa, 1680 East-West Road, Honolulu, HI, U.S.A.*

<sup>(3)</sup>*Jet Propulsion Laboratory, California Institute of Technology, 4800 Oak Grove Drive, Pasadena, CA, U.S.A.*

<sup>(4)</sup>*Saraniasat, Los Angeles, CA, U.S.A.*

## ABSTRACT

The HyTI (Hyperspectral Thermal Imager) mission, funded by NASA’s Earth Science Technology Office InVEST (In-Space Validation of Earth Science Technologies) program, will demonstrate how high spectral and spatial long-wave infrared image data can be acquired from a 6U CubeSat platform. The mission will use a spatially modulated interferometric imaging technique to produce spectro-radiometrically calibrated image cubes, with  $\sim 25$  channels between 8-10.7  $\mu\text{m}$ , at  $13\text{ cm}^{-1}$  resolution, at a ground sample distance of  $\sim 60\text{ m}$ . Pre-launch measurements indicate single channel NE $\Delta$ Ts of  $<0.2\text{ K}$ . The small form factor of HyTI is made possible via the use of a no-moving-parts Fabry-Perot interferometer, and a cryogenically-cooled HOT-BIRD (High Operating Temperature Barrier InfraRed Detector) focal plane array. The value of HyTI to Earth scientists will be demonstrated via on-board processing of the raw instrument data to generate L1 and L2 products, with a focus on rapid delivery of data regarding volcanic degassing, and land surface temperature. HyTI was successfully launched onboard SpX-30 on 21 March 2024, and will be deployed from the International Space Station on 18 April 2024. Nominal mission lifetime is expected to be 12 months.

## 1. INTRODUCTION

Since the launch of the Landsat 4 Thematic Mapper, scientists interested in studying the long-wave infrared (LWIR) thermal properties of Earth’s surface, atmosphere, and water bodies at high-to-moderate resolution have been limited to making measurements at a 60-120 m ground sample (e.g. Landsat TM, ETM+, and the most recent iteration, the Landsat 8 and Landsat 9 TIIRS sensor), in no more than five spectral bands (e.g., Terra ASTER). It can be argued that the ECOSTRESS mission [1] currently operating on the International Space Station represents the state-of-the-art for orbital moderate resolution thermal remote sensing, via the acquisition of five channels in the 8-12  $\mu\text{m}$  interval at  $69 \times 38\text{ m}$  resolution. Operational acquisition of high spatial and spectral resolution LWIR data from Earth orbit would yield an hitherto unattainable measurement record for Earth scientists. Applications include mapping the chemistry of rocks and minerals exposed at Earth’s surface [2], the composition of volcanic gas and ash plumes [3], and quantifying soil moisture content and evapotranspiration [4]. The HyTI mission will demonstrate how recent innovations in LWIR imaging

technologies can be combined to provide high spatial and spectral resolution LWIR image data from a 6U platform.

## 2. THE HYTI PAYLOAD AND IMAGE MEASUREMENT TECHNIQUE

The HyTI imager is a novel, no-moving-parts hyperspectral imager that was originally developed using funding from DARPA and NASA. Light from the scene is focused by a refractive lens and passed through a Fabry-Perot interferometer mounted directly above the focal plane array within the integrated dewar cooler assembly (IDCA).

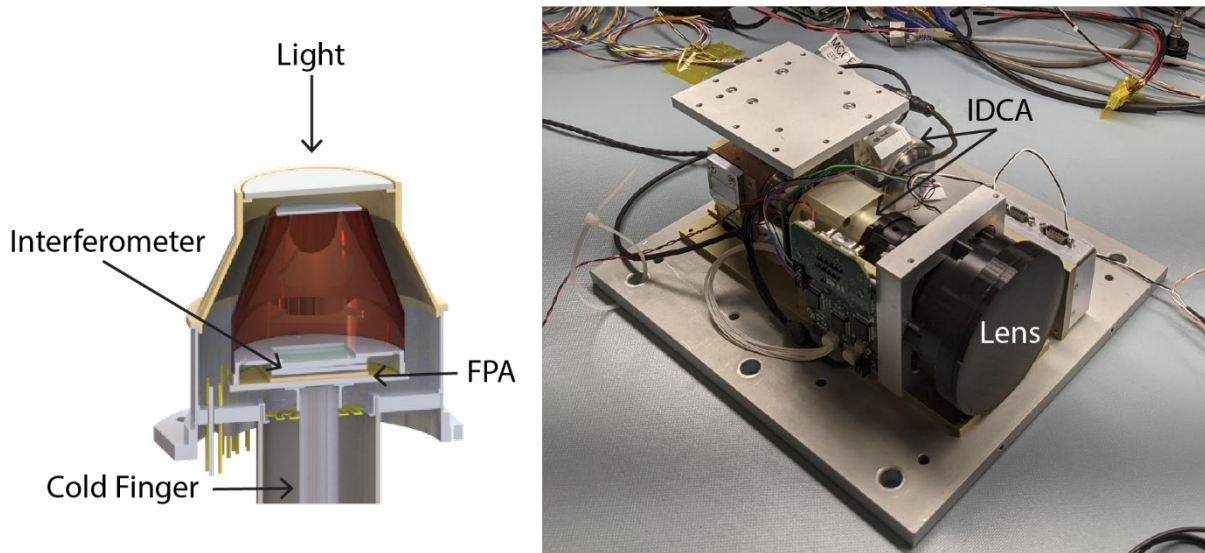


Figure 1. Right: HyTI payload. Left: detail of the HyTI interferometer and FPA within the dewar

Forward motion of the platform allows interferograms of targets on the ground to be reconstructed, as each ground target is imaged at a succession of optical path differences as the fixed interference pattern is pushed along the ground in the in-track flight direction. Figure 2 illustrates the process. The Fabry-Perot interferometer consists of two pieces of germanium (AR coated), with a sloped air-gap between. Reflection, transmission and eventual recombination of rays that traverse this gap produces interference that can be sampled at the array. The slope ensures that optical path difference (hence fringe period) varies linearly across the air gap. A single frame of data (top left, Figure 2) records light emitted from each scene element modulated at one OPD per column of the array, and the broad dark vertical stripe on the right hand side of these images denotes the point at which the pieces of Ge are contacted, where no modulation takes place, with interference fringes extending from this point. As such, each column of the array contains a portion of an interferogram for each scene element in each column. By translating the interference across the scene (using forward motion of the platform; HyTI is a pushbroom imager, and the design frame rate oversamples in the interference pattern in the in-flight direction) light emitted from each scene element is modulated at each OPD. After co-registration of the image frames, standard Fourier Transform techniques [5] are used to produce a spectro-radiometrically calibrated image cube. The spectral resolution of an interferometer is given by the ratio of the cut-off frequency to the number of samples in a single-sided interferogram [6], and the fringe periodicity (number of samples) for HyTI is proportional to the design slope of the air-gap (although system f-number provides an ultimate constraint on the spectral resolution achievable with this design [7, 8]).

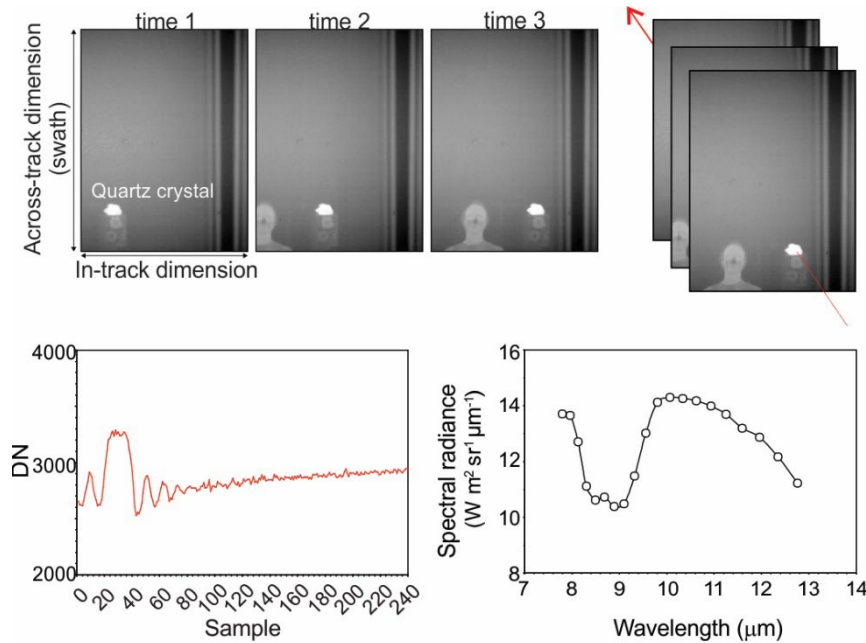


Figure 2. Top left: images of a quartz cube acquired at successive time steps, as the interference pattern is scanned across the scene. Co-registration of the frames (top right) allows an interferogram (lower left) to be obtained for each pixel in the image cube, from which a radiance spectrum (lower right) can be retrieved.

HyTI allows for high spatial and spectral resolution LWIR imaging by combining the multiplex advantage common to all interferometers with the sensitivity of JPL's Barrier Infra-Red Detector FPA technology [9]. Based on III-V compound semiconductors, the BIRD detectors are low cost (high yield), high-performance FPAs with excellent uniformity and pixel-to-pixel operability. These antimony (Sb) compound-based BIRD detectors outperform existing TIR detectors including Quantum Well Infrared Photodetectors (QWIPs). To achieve acceptable dark current levels, the FPA will be maintained at a temperature of 68 K, although our pre-flight measurements indicate that requirements are met if the FPA runs at 72 K. HyTI uses an FPA of  $640 \times 512$  elements, but the HyTI ROIC cannot read the entire array at the required frame rate (139 Hz), and so HyTI will use a window of 256 detectors to define the field of view (swath), with 320 detectors used to sample the interference pattern generated by the Fabry-Perot interferometer (the in track direction). A frame rate of  $>139$  Hz allows for oversampling in the in-track dimension at orbital velocity.

### 3. HYTI DATA AND PRE-LAUNCH IMAGING RESULTS

From an orbital altitude of  $\sim 400$  km (i.e., ISS orbit) the design ground sample distance of HyTI will be  $\sim 60$  m (Figure 3). 25 spectral samples between 8-10.7  $\mu\text{m}$  will be acquired (spectral resolution of  $13 \text{ cm}^{-1}$ ). HyTI will have no on-board calibration targets, given the volume constraints of the 6U platform. T2SLS detectors are very stable in time [10]. Calibration will be via intermittent deep-space looks (to calculate radiometric offsets) with pre-launch look-up tables of gain vs FPA temperature vs integration time. Validation will use intermittent Lunar scans, and vicarious calibration using Landsat and ASTER images.

Pre-launch measurements indicate that narrow-band NEDTs meet requirements (i.e.,  $<0.35\text{K}$ ). Figure 4 shows test data acquired by HyTI for test targets. For a near-uniform spectral targets (a block of quartz), pixel-to-pixel repeatability is excellent.

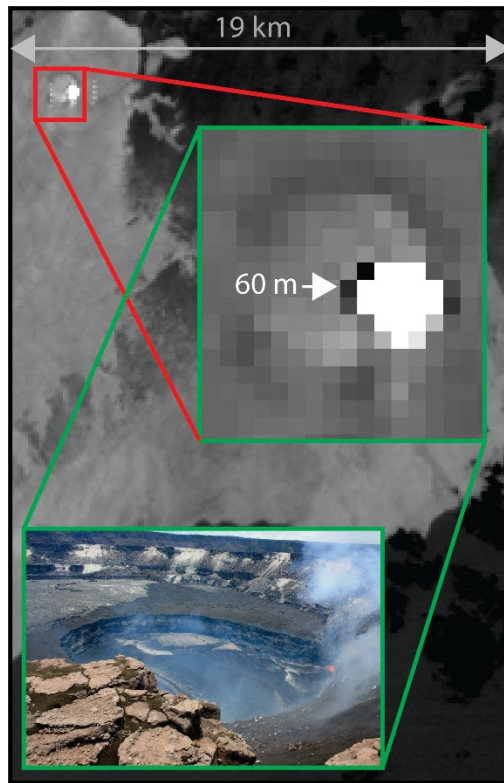


Figure 3. Illustration of HyTI image swath and ground resolution, using a Landsat ETM+ band 6 image of Kilauea volcano, Hawai'i.

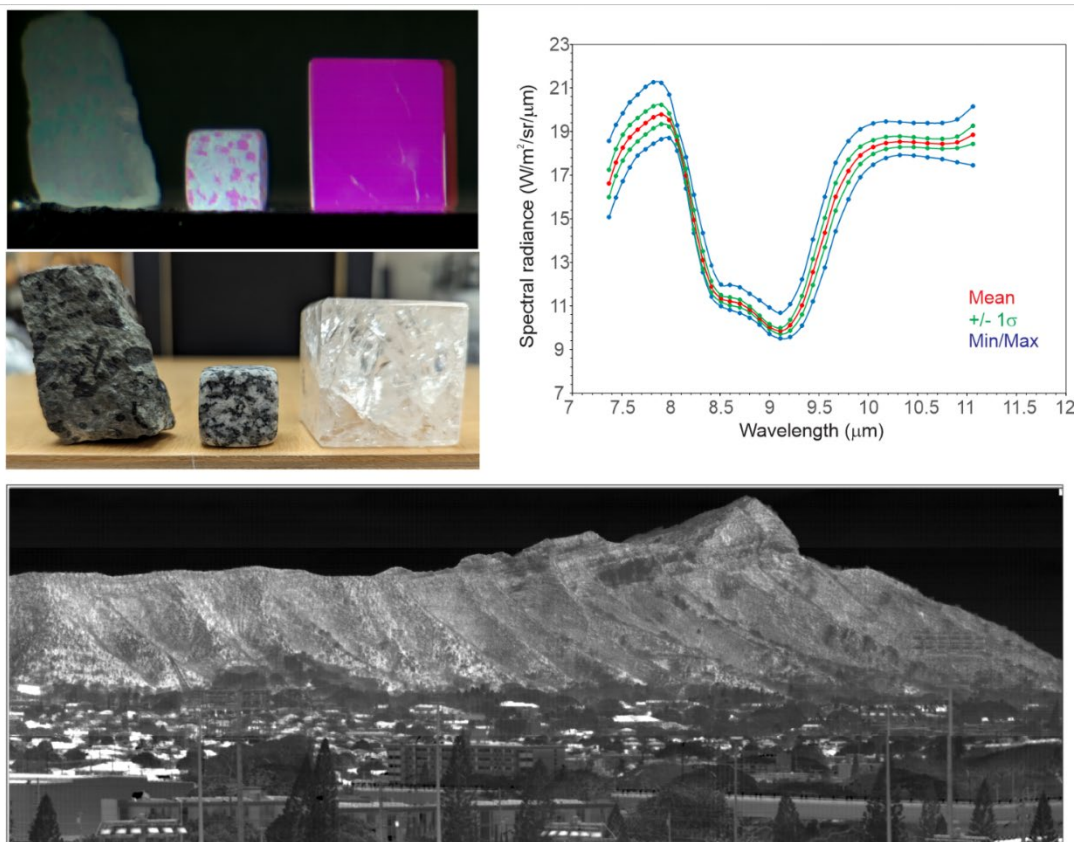


Figure 4. Top: false color triplet of rock/mineral targets acquired by HyTI. On the right are the spectra of ~10,000 pixels for the quartz cube (magenta block in the image).

#### 4. SUMMARY

The HyTI (Hyperspectral Thermal Imager) mission will demonstrate how high spectral and spatial long-wave infrared image data can be acquired from a 6U CubeSat platform. The mission will use a spatially modulated interferometric imaging technique to produce spectro-radiometrically calibrated image cubes, with 25 channels between 8-10.7  $\mu\text{m}$ , at a ground sample distance of  $\sim 60$  m. The HyTI performance model indicates narrow band NE $\Delta$ Ts of  $<0.2$  K. The small form factor of HyTI is made possible via the use of a no-moving-parts Fabry-Perot interferometer, and JPL's cryogenically-cooled BIRD FPA technology. The HyTI satellite was launched on board SpX-30 on 21 March 2024 (Figure 5), and will be deployed from the International Space Station on 18 April 2024.

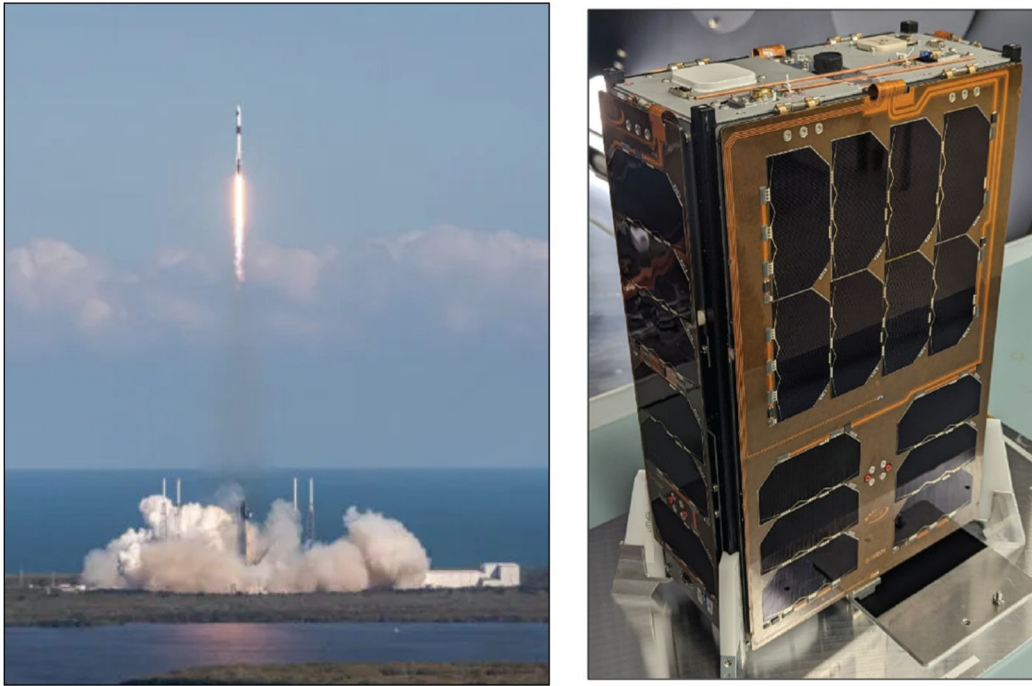


Figure 5. Left: SpX-30 launch, March 21, 2024. Right: HyTI spacecraft.

#### 5. ACKNOWLEDGEMENTS

HyTI is funded by NASA's Earth Science Technology Office InVEST (In-Space Validation of Earth Science Technologies) program element (grant number 80NSSC18K1601). The research was partly carried out at the Jet Propulsion Laboratory, California Institute of Technology, under a contract with the National Aeronautics and Space Administration

#### 6. REFERENCES

- [1] Fisher, J. B., Lee, B., Purdy, A. J., Halverson, G. H., Dohlen, M. B., Cawse-Nicholson, K., et al. (2020). ECOSTRESS: NASA's Next Generation Mission to measure evapotranspiration from the International Space Station. *Water Resources Research*, 56, e2019WR026058. <https://doi.org/10.1029/2019WR026058>
- [2] Hall, J. L., Hackwell, J. A., Tratt, D. M., Warren, D. W. and Young, S.J (2008). Space-based mineral and gas identification using a high-performance thermal infrared imaging spectrometer. *Proceedings of SPIE*, 7082, 70820M.

- [3] Gabrieli, A., Porter, J., Wright, R., and Lucey, P (2017). Validating the accuracy of SO<sub>2</sub> gas retrievals in the thermal infrared (8-14 μm). *Bulletin of Volcanology*, 80, <https://doi.org/10.1007/s00445-017-1172-2>, 2017.
- [4] Anderson, M. C., Norman, J. M., Kustas, W. P., Houborg, R., Starks, P. J., and Agam, N. (2008). A thermal-based remote sensing technique for routine mapping of land-surface carbon, water and energy fluxes from field to regional scales. *Remote Sensing of Environment*. 112 (12), 4227-4241.
- [5] Mertz, L. (1965). *Transformations in Optics*. Wiley.
- [6] Griffiths P.R. and DeHaseth, J.A. (1986). *Fourier Transform Infrared Spectrometry*. Wiley.
- [7] Lucey, P. G., and Akagi, J. (2011). A Fabry-Perot interferometer with a spatially variable resonance gap employed as a Fourier transform spectrometer. *Proceedings of SPIE*, 8048, 80480K-1.
- [8] Lucey, P.G., Hinrichs, J.L., and Akagi, J. (2012). A compact LWIR hyperspectral system employing a microbolometer array and a variable gap Fabry-Perot interferometer employed as a Fourier transform spectrometer. *Proceedings of SPIE*, 8390, 83900R-1.
- [9] Ting, D., Soibel, A., Khoshakhlagh, A., Rafol, S. B., Keo, S. A., Höglund, L., Fisher, A. M., Luong, E. M., and Gunapala, S. D. (2018). Mid-wavelength high operating temperature barrier infrared detector and focal plane array. *Applied Physics Letters*, 113, 021101.
- [10] Arounassalame, V., Guenin, M., Caes, M., Hoglund, L., Costard, E., et al. (2021). Robust Evaluation of Long-Term Stability of an InAs/GaSb Type II Superlattice Midwave Infrared Focal Plane Array. *IEEE Transactions on Instrumentation and Measurement*, 70, pp.5001108. {10.1109/TIM.2020.3024406}.